Mapping of impaired functional connectivity during memory phases in Alzheimer's disease and its association with cortical β-amyloid

Binyin Li
Shanghai Jiao Tong University Medical School Affiliated Ruijin Hospital https://orcid.org/0000-0003-1953-382X

Miao Zhang
Shanghai Jiao Tong University Medical School Affiliated Ruijin Hospital

Guanyu Ye
Shanghai Jiao Tong University Medical School Affiliated Ruijin Hospital

Liche Zhou
Shanghai Jiao Tong University Medical School Affiliated Ruijin Hospital

Guiying He
Shanghai Jiao Tong University Medical School Affiliated Ruijin Hospital

Xiaozhu Lin
Shanghai Jiao Tong University Medical School Affiliated Ruijin Hospital

Hongping Meng
Shanghai Jiao Tong University Medical School Affiliated Ruijin Hospital

Xinyun Huang
Shanghai Jiao Tong University Medical School Affiliated Ruijin Hospital

Wangxi Hai
Shanghai Jiao Tong University Medical School Affiliated Ruijin Hospital

Shengdi Chen
Shanghai Jiao Tong University Medical School Affiliated Ruijin Hospital

Biao Li
Shanghai Jiao Tong University Medical School Affiliated Ruijin Hospital

Jun Liu (✉ jly0520@hotmail.com)
https://orcid.org/0000-0001-8300-8646

Research

Keywords: β-amyloid, functional MRI, memory retrieval

Posted Date: July 2nd, 2020

DOI: https://doi.org/10.21203/rs.3.rs-39379/v1

Abstract

Background: Amnesia in Alzheimer's disease (AD) could be due to disrupted encoding, consolidation dysfunction, or an impairment in the retrieval of stored memory information. The different memory phases relate with different parts of functional brain systems.

Methods: We combine task functional magnetic resonance imaging and amyloid positron emission tomography in 72 participants (36 AD and 36 controls), to investigate the relationship between memory performance, memory phase-locked functional connectivity, and cortical β-amyloid deposition.

Results: We found that AD was mainly characterized by decreased functional connectivity in a new data-driven Network composed of regions from default mode network, limbic network and frontoparietal network during the memory maintenance and retrieval phase. Within the Network, AD had more regions with reduced connectivity during the retrieval phase than other phases, locating mainly in the medial prefrontal cortex, posterior cingulate cortex, middle temporal and inferior parietal cortex of left hemisphere. Furthermore, functional connectivity in the Network related to memory performance. Crucially, the magnitude of the Network connectivity reduction during retrieval negatively correlated with mean cortical β-amyloid, and this relationship mediated the relationship between cortical β-amyloid and memory performance.

Conclusions: Our findings show that memory deficiency in AD relates with decreased connectivity in specific network and cortical β-amyloid only during retrieval phase. These findings help to map impaired functional connectivity during memory phases and explain the relationship between memory deficiency and cortical β-amyloid.

Background

Alzheimer's disease (AD) is marked by prominent memory deficiency in the early stage. It is controversial whether the observed amnesia is due to disrupted encoding or consolidation of episodic information, or an impairment in the retrieval of stored memory information. Several studies have suggested that the ineffective encoding of new information in the brain triggers episodic memory deficits (1, 2), while more evidence supported retrieval deficit in early AD (3–5). Transgenic AD mouse models also suggested that direct activation of hippocampal memory engram cells resulted in memory retrieval, revealing a retrieval, rather than a storage impairment in early AD (6).

Many studies have been conducted to understand where and how memory is stored and retrieved. Conventionally, it is suggested that memory is stored as multiple traces in hippocampal neurons. In older adults, episodic memory processing-related medial temporal lobe activation was negatively associated with higher global β-amyloid (Aβ) levels (7, 8). In early AD, the inability to encode and retrieve memory is present at the earliest stages of the disease and deteriorates during disease course (9). Recent evidence indicates that there are specialized memory engrams responsible for the storage and the retrieval of different memory types, as reviewed here (10). The engram cells work with neocortex such as the

cingulate cortex and medial prefrontal cortex. Furthermore, some cortex neurons, which are not normally the engram cells, can have engram function during memory retrieval (11).

Together, these findings suggest that neural interactions might exert an influence on memory retrieval, and thus affect memory performance in AD. However, this hypothesis has not been tested in humans. Besides, as the Aβ is regarded as the key marker of the “Alzheimer continuum” (12), it is necessary to clarify the adverse effect of cortical deposition on memory-related neural function along the disease continuum.

To address this caveat in the literature, we characterized detailed alterations in cortical connectivity networks during different memory phases (encoding, maintenance and retrieval) in 36 AD and 36 non-demented participants by task functional magnetic resonance imaging (fMRI). In the same participants, we measured cortical Aβ deposition using positron emission tomography (PET). In addition, we investigated how increasing levels of Aβ pathology in cortex affect cortical connectivity networks. To assess the clinical relevance of the observed functional alterations, we related them to measures of memory performance.

Our primary hypothesis was that AD functional connectivity changes within specific cortical networks during memory retrieval. The cortical Aβ deposition would correlate with the functional connectivity, and this relationship would mediate the influence of cortical Aβ on memory performance. The findings further our understanding of the mechanisms underlying memory deficiency in AD by Aβ pathology on critical memory systems and suggest mapping of functional connectivity as a therapeutic target.

Materials And Methods

Participants

Participants with clinically diagnosed AD were recruited from the Memory Clinic at Shanghai Jiao Tong University School of Medicine affiliated Ruijin Hospital. AD was diagnosed using the syndromal categorical cognitive staging scheme and positive amyloid deposition by PET, based on the National Institute on Aging-Alzheimer’s Association (NIA-AA) workgroups (12). Based on cognitive status, neuropsychologic test performance, and Aβ positivity determined by agreement between one nuclear medicine specialist and one memory-disorder specialist, 36 AD participants were included in this study. The Aβ- normal controls were recruited from one community without dementia. They were assessed by the identical neuropsychological tests as AD. Structural, functional MRI and Aβ PET data were also acquired from these participants.

All participants were initially screened by the Mini-Mental State Examination (MMSE, Chinese Version) (13), global clinical dementia rating (CDR > 0.5 for AD diagnosis), Zung Self-rating Anxiety Scale, Self-rating Depression scale and activity of daily living questionnaire. Demographics included sex, age, education level, occupation, concomitant diseases, and medications. After inclusion, each participant underwent neuropsychological tests that included the Beijing version of the Montreal Cognitive

Assessment (MoCA) and the Chinese version of Addenbrooke's Cognitive Examination-Revised (ACER) with subtests of memory, language, attention, fluency and visual-spatial processing (14).

The present study was approved by the ethics committee, Shanghai Jiao Tong University affiliated Ruijin Hospital, China. All participants in the study or their caregivers signed written informed consent after fully understanding the procedure involved.

Task Design In Fmri

The task was an event-related design, with a total of 34 encoding objects and 56 retrieval objects (Fig. 1). During the encoding phase, the participants studied 34 unique objects [3 × 3 degrees of visual angle], which were presented for 2 s and had 2–6 s randomized interstimulus intervals. In the following 2-min maintenance phase, the screen was blank, and no stimulus was presented. Then in the retrieval phase, there were 56 test trials presenting objects with the same visual angle. The objects were presented sequentially, followed by 2–6 s interstimulus intervals. The participants were asked to judge whether the objects were “old” (studied) or “new” (unstudied). The participants had up to 4 s to respond. Among these trials, half presented old (studied) objects, and half presented new (unstudied) objects. Task accuracy was defined as the percentage of the correct answer in 56 recognition objects.

The participants viewed an MRI-compatible liquid crystal display monitor via a mirror mounted to the head coil. All responses were recorded by an MRI-compatible optical mouse. The order of object presentation was randomized across all participants. The duration of the task fMRI slightly varied from 11 to 13 min based on interstimulus interval randomization and reaction times.

Acquisition Of Mr And Pet Images

MRI data were acquired on a whole-body PET/MR scanner (Biograph mMR; Siemens Healthcare, Erlangen, Germany) with a standard 8-channel head coil. Whole-brain functional images were acquired during the tasks, with a 3000-ms repetition time (TR), a 30-ms echo time (TE), a 192 × 192 mm field of view (FOV), a 90° flip angle, 35 slices, and voxel size of 3.0 × 3.0 × 3.0 mm^3 (each measurement consisted of 260 acquisitions in interleaved mode with a total scan time of 13 min and 8 s).

PET scans using an ^{18}F florbetapir (AV45) tracer to image Aβ were performed on the same day of fMRI. The participants received an IV injection of ^{18}F florbetapir at a mean dose of 3.7 MBq/kg body weight after finishing the task fMRI. Static AV45-PET data were acquired in sinogram mode for 15 min using the following parameters: 128 slices (gap, 0.5 mm) covering the whole brain; FOV, 500 mm; matrix size, 344 × 344; voxel size, 2.6 × 2.6 × 3.1 mm^3, reconstructed with high-definition (HD) PET (21 subsets, 4 iterations) and post-filtered with an isotropic full-width half-maximum (FWHM) Gaussian kernel of 2 mm. The T1-weighted 3-dimensional structural image was simultaneously acquired with TR = 1900 ms, TE = 2.44 ms

and 192 slices covering the whole brain. Attenuation correction for PET was performed using MR-based attenuation maps derived from a dual-echo Dixon-based sequence.

Fmri Activation Analysis: Standard Univariate Analysis

Functional and T1 MRI data were preprocessed by Freesurfer 6.0 and FsFast version 5.0 (surfer.nmr.mgh.harvard.edu). The preprocessing pipeline for fMRI included templating from the middle time point of raw functional data, masking, functional-anatomical registration, motion correction, slice-timing, and resampling the raw time series to the left and right hemispheres. Quality control of functional-anatomical registration was performed by both automatic rating from Fressurfer and visual inspection. Two-dimensional spatial smoothing was performed for surface data with a Gaussian kernel of 5-mm in FWHM.

The encoding and retrieval phases were evaluated separately using the surface-based stream. For the first-level general linear model (GLM) analysis, contrasts (encoding stimulus against interstimulus rest; recognition stimulus against interstimulus rest) were calculated by the Gamma hemodynamic response function within the cortical surface at each voxel. We inspected each case after the first-level analysis by visualization to ensure that they registered well with the FreeSurfer average surface (common space). All cases were concatenated for further analysis.

In the second-level analysis, task accuracy-related activation maps were generated in all participants by GLM with accuracy as a regressor. Significant clusters were computed after permutation resampling by bootstrapped Monte Carlo simulations (10,000 iterations) at $p = 0.001$ to correct for multiple comparisons across all brain voxels. We finally had clusters with that size or larger during the simulation and corrected the threshold to $p < 0.05$ (15). The coefficients of activation were extracted after mapping on the native surface using an inverse affine transform for further analysis.

Fmri Phase-locked Functional Connectivity

For functional connectivity, we re-preprocessed fMRI by pipeline implemented in the CONN toolbox (version19.c) (https://www.nitrc.org/projects/conn) within MATLAB, similar to the previous study (16). This pre-processing included slice timing correction, realignment of functional scans and normalization to MNI space and spatial smoothing (Gaussian kernel of 8 mm FWHM). In the denoising step, linear regression was used to remove the influence from: (1) Blood oxygen level-dependent (BOLD) signal from the white matter and CSF voxels (five components each, derived using the anatomical component-based correction implemented using the ART toolbox), (2) six residual head motion parameters and their first order temporal derivatives, (3) scrubbing of artifact/outlier scans, and (4) effect of task-condition using event regressors (encoding and retrieval stimulus) convolved with the hemodynamic response function. Finally, the denoising step included temporal bandpass filtering (0.008–0.09 Hz), and linear detrending of the functional time course.

Following pre-processing, we extracted individual phase-locked (encoding, maintenance and retrieval) averaged time-series from 200 cortical nodes defined by the Schaefer fMRI atlas, which is based on a data-driven fMRI brain parcellation (17). The 200 nodes can be assigned to seven *priori* functional networks, including visual network, somatomotor network, dorsal attention network (DAN), ventral attention network (VAN), limbic network, frontoparietal network (FPN) and default mode network (DMN). This atlas is well-suited for joint analyses of pathological PET in the cortex and fMRI, since the nodes cover the neocortex and are adaptive from volume to surface. As described before, we performed the connectivity analysis on the time series after removing event-related effects (16).

Data-driven Detection Of Empirical Networks From The Maintenance Phase

The functional connectivity between two brain regions (nodes) was defined as the Fisher z-transformed Pearson's correlation coefficient between the BOLD time-series in each region. We used the functional connectivity measures in the maintenance phase from the control group to generate an undirected weighted covariance matrix, C, where c_{ij} represents the Fisher z-transformed Pearson's correlation coefficient between node i and j (i.e. edge strength between nodes). After setting negative weights to 0, we used the Louvain algorithm (implemented in the MATLAB Brain Connectivity Toolbox, https://sites.google.com/site/bctnet/) to get the control group-level empirical networks (10) in the maintenance phase (Supplementary material).

We restricted the community detection analysis to the 136 nodes allocated to the limbic network, DMN, DAN, VAN and FPN (16), as defined by the Schaefer atlas. Given the stochastic nature of the Louvain algorithm, we used a consensus clustering approach to ensure the robustness of the final community structure by agreement.m and consensus_und.m functions in the Brain Connectivity Toolbox (18–20) (see Supplementary material for details). Finally, these nodes were clustered into three new empirical networks from controls.

Functional Connectivity Statistical Analysis In Each Memory Phase

The new empirical networks from controls during the maintenance phase were used to group nodes for all participants in each memory phase. The mean functional connectivity within/between the new networks was compared between groups in each phase, respectively. We also measured the relationship between cognition performance and mean functional connectivity within/between each empirical network.

Furthermore, the network component analysis was performed using node-wise connectivity maps within the network that showed group differences in mean functional connectivity. For functional connectivity in

each phase, it entered into a group analysis gauging differences in AD and controls using codes similar to the NBS (v1.2) algorithm (21). Different from the traditional NBS, all the links' *t*-values were calculated in a general linear model after regressing out age and sex (22). Applying a two-sided suprathreshold, the differences in node-node functional connectivity between two groups would be visualized as binary outcomes in each memory phase (Supplementary material).

We also gauged the BOLD series' information content using an entropy measure for discrete time series called sample entropy (23) (setting embedding dimension m = 2 and the range in SD from all time series). The measure should be higher for time series with lower predictability and random disorder, and conversely reduced for more ordered and predictable time series (24).

Pet Image Analysis

For ^{18}F-florbetapir (AV45) PET, we employed an automatic pipeline to extract cortical standardized uptake value ratios (SUVRs) implemented in PETSurfer FreeSurfer 6.0 (https://surfer.nmr.mgh.harvard.edu/fswiki/PetSurfer). In detail, structural T1 images were used to creates a high-resolution segmentation to run the following partial volume correction (PVC) methods. The PET/anatomical image registration was then performed and visually checked. To minimize partial volume effect from cortical atrophy in AD, we applied the Symmetric Geometric Transfer Matrix as PVC methods for the following ROI analysis (25), using the cerebellum cortex as the reference region. Surface-based SUVR maps were smoothed on the 2-dimensional surface by a Gaussian kernel of 5 mm in full width at half maximum. Again, we applied the 200-parcellation from Schaefer fMRI atlas that had been adapted from volume to cortex surface and extracted cortical SUVRs.

Statistical analysis

Statistical analyses were performed with R (Version 3.6.2). AD and controls were compared using independent t-test or Chi-square test for continuous or nominal variables, respectively. We used Pearson's correlation coefficient to test for relationships between phase-locked connectivity within/between empirical networks, cortical amyloid and cognitive performance. All significant results were double-checked by the *RVAideMemoire* package in R, performing a permutation Pearson's product-moment correlation test or Student's t-test with 10,000 permutations.

To control for age, education and sex as covariates, we further used linear regressions with network connectivity and cortical amyloid as predictors of cognitive performance (variables were normalized into z scores). We tested the hypothesis that cortical amyloid influences memory performance by modulating cortical network connectivity with a mediation analysis using the 'mediation' package, implementing a nonparametric bootstrap method with bias-corrected and accelerated confidence intervals and 10,000 simulation draws. All tests were 2 tailed, and values of corrected $p < 0.05$ were considered statistically significant unless specified otherwisea. Supplementary Fig. 1 summarizes our analysis approach.

Results

Participants and task-related activation

A total of 36 AD and 36 cognitively unimpaired controls satisfied the aforementioned inclusion criteria. The two groups were matched in age, education, and sex (Table 1), and AD had worse cognitive performance in all cognitive domains assessed by the MMSE, MoCA, and ACER as expected. Additionally, in the fMRI task, the AD group had lower accuracy than the control group. Furthermore, task accuracy had significant correlations with the MoCA ($R = 0.610$, $p < 0.001$), the ACER ($R = 0.652$, $p < 0.001$), and more strongly with ACER memory scores ($R = 0.696$, $p < 0.001$).

Table 1
Demographic and clinical characteristics

	AD	Control	P
Number	36	36	
Sex (M/F)	17/19	15/21	0.232
Age	68.78 ± 7.63	69.05 ± 7.11	0.778
Education	12.08 ± 2.53	13.27 ± 2.83	0.076
MMSE	19.88 ± 5.49	28.05 ± 1.86	< 0.001
MoCA	15.36 ± 6.71	26.54 ± 2.41	< 0.001
ACER	56.50 ± 18.8	89.30 ± 6.73	< 0.001
Attention	11.61 ± 3.81	17.02 ± 1.13	< 0.001
Memory	15.42 ± 4.92	21.61 ± 3.73	< 0.001
Fluency	6.19 ± 3.38	10.11 ± 2.15	< 0.001
Language	19.00 ± 5.74	24.97 ± 1.68	< 0.001
Visuospatial	11.13 ± 4.69	15.72 ± 0.55	< 0.001
Task accuracy	0.23 ± 0.09	0.62 ± 0.38	< 0.001
Cortical thickness	2.28 ± 0.15	2.39 ± 0.11	< 0.001

Data are expressed as the mean ± standard deviation. Two-sample independent t-test was conducted to test between-group differences, and p values were corrected by permutation. The Chi-square test was used for categorical variables. ACER = Addenbrooke's Cognitive Examination-Revised; MoCA = Montreal Cognitive Assessment.

As expected, in a standard fMRI GLM analysis for activation, there were activations in widespread visual, frontoparietal and attention networks of the left hemisphere (voxel-wise $p < 0.001$, cluster-wise corrected $p < 0.05$ after correction by randomized permutation simulator, Table 2). Besides visual network, the most

prominent activation was in the left superior frontal cortex (Talairach Montreal Neurological Institute (MNI305) coordinates: -5.8, -7.8, 53.5; $p = 0.001$, activation $\beta = 5.429$, lower right in Fig. 2). The activation was located in the ventral attention network of the Schaefer functional atlas, and mainly correlated with ACER memory ($R = 0.435$, $p < 0.001$), followed by ACER ($R = 0.348$, $p < 0.001$) and MoCA ($R = 0.373$, $p < 0.001$). In the encoding phase, there was no significant linear or quadratic relationship between neural activation and task accuracy when this variable was used as a regressor in a second-level voxel-wise analysis.

Table 2
Whole-brain activation results for task accuracy regressor

Activation clusters Left hemisphere	**Peak**		**Talairach MNI Coordinates (mm)**		
	Activation β	P_{corr}	x	y	z
Lateral occipital	5.56	0.001	-27.1	-93.2	9.4
Superior frontal	5.429	0.001	-5.8	-7.8	53.5
Inferior temporal	6.366	0.004	-40.2	-61.8	-6
Caudal middle frontal	5.026	0.005	-36.1	7.8	35.3
Supra marginal	4.982	0.005	-53.3	-19.7	21.4
Lateral occipital	5.001	0.005	-25	-82.4	-11
Fusiform	4.888	0.007	-39.7	-54.5	-20.1
Pericalcarine	4.818	0.013	-9.8	-98.6	4.6
Lingual	6.081	0.016	-10.7	-90	-9.4
Fusiform	4.86	0.019	-32.6	-52.3	-9.8
Parsopercularis	6.629	0.044	-43.4	7.1	18
Lateraloccipital	3.391	0.044	-35.3	-81.4	-14.6

Activation peaks present in the significant clusters at the whole-brain threshold of $P < 0.05$ (corrected by permutation resampling of bootstrapped Monte Carlo simulations, 10,000 iterations). Anatomical labeling corresponds to the peak 'Talairach' MNI coordinate, illustrated here: https://surfer.nmr.mgh.harvard.edu/fswiki/CoordinateSystems. MNI = Montreal neurological institute.

Empirical Networks During Maintenance From Controls

To investigate memory phased-locked functional connectivity changes within task-relevant cortical networks, we first used a data-driven community detection algorithm (18, 26) to partition the cortex into 3 group-level networks (Network 1, 56 nodes; Network 2, 50 nodes; Network 3, 30 nodes), using the time

series during the maintenance phase in the control group (see Fig. 2 for the resulting partition). All three empirical networks were visually symmetrical in the cortex. The ‘empirical’ Network 1 node assignments overlapped with the *a priori* network assignments from the Schaefer functional atlas in DMN, limbic network and FPN. The Network 2 mainly overlapped with dorsal and ventral attention networks, as well as the spatial activation maps from the standard fMRI activation analysis. The Network 3 generally included regions assigned to FPN and its adjacent DMN regions.

Left top, right top and left down cortical mapping illustrated nodes of the three empirical networks identified by the community detection algorithm during the maintenance phase, colored by a *priori* network assignments from the Schaefer cortical parcellation. Network 1 is mainly composed of DMN, limbic network and FPN, and Network 2 consists of DMN and FPN. The Network 3 generally includes DAN and VAN. The right down is the surface maps of the activated cortex in the retrieval phases related to accuracy. The border on the surface indicated the network identical to the above Schaefer cortical parcellation. The activation is observed in the region of VAN. DMN = default mode network; FPN = frontoparietal network; DAN = dorsal attention network; VAN = ventral attention network.

For each participant, we defined the phase-locked (encoding, maintenance, retrieval) functional connectivity within/between the Network 1–3 by functional connectivity strength (Fisher z-transformed r-value) in the edges connecting nodes in the three Networks. Thus each participant had three phase-specific functional connectivity matrices, and their mean matrices for AD and control group were shown in Fig. 3.

Reduced Network 1-Network 1 functional connectivity in AD only during the retrieval phase. The first and second columns: Mean functional connectivity in each task phase of network edge (node-node connection) in the AD and controls. Each edge (cell of the matrix) represents the functional connectivity strength (Fisher z-transformed r-value) within and between the Network 1–3. The third column: The difference of functional connectivity in each task phase of each network edge (node-node connection) between the AD and controls. Black lines indicate the boundary separating nodes allocated to the empirical Network 1–3.

Network 1 Connectivity Is Reduced In Ad

We first investigated group differences between the AD and control in the mean functional connectivity within/between the three empirical networks. The AD group had significantly reduced connectivity within Network 1 during maintenance (0.205 vs 0.236, p = 0.040) and retrieval (0.159 vs 0.183, $p = 0.017$). No difference in functional connectivity within Network 1 was observed in the encoding phase. We investigated the specificity of group differences in phase-locked network connectivity in two additional analyses. First, there was no solid group difference in network functional connectivity averaged over each memory phase in the Network 2 ($p = 0.081, 0.088, 0.449$ for encoding, maintenance and retrieval) and Network 3 ($p = 0.073, 0.914, 0.934$ for encoding, maintenance and retrieval). Second, there was also no

group difference in functional connectivity during each memory phase in the networks' interaction (i.e. Network 1-Network 2, Network 3-Network 2, all $p > 0.250$).

Relationship Between Network 1 Connectivity And Memory

There were significant positive correlations between the Network 1-Network 1 connectivity and ACER memory performance in encoding, maintenance and retrieval phases ($R = 0.249, 0.318, 0.304$; $p = 0.032, 0.004, 0.008$; df = 70), indicating that participants who showed the greatest reduction of functional connectivity within the Network 1 also showed the worst memory performance (Fig. 4). We also observed similar positive relationships between memory performance and connectivity within the Network 2 during maintenance and retrieval phase, as well as Network 3 during maintenance. These results were robust to the permutation test at the level of $p < 0.05$. There was no similar relationship for connectivity between the networks in any phase.

Memory scores in ACER were associated with Network 1-Network 1 functional connectivity in the encoding, maintenance and retrieval phase, while only associated with Network 2-Network 2 functional connectivity in the maintenance and retrieval phase. No other associations were observed. R and P_{corr} represented correlation coefficient and significance across two groups. P_{corr} in the correlation analysis was corrected by 10,000 permutations. The grey zone around blue lines represents the 95% confidence interval for predictions from the linear model. ACER_M = Addenbrooke's Cognitive Examination-Revised Memory; N1_1 = Network 1-Network 1; N2_2 = Network 2-Network 2; N3_3 = Network 3-Network 3; N1_3 = Network 1-Network 3; N2_3 = Network 2-Network 3. R = Retrieval; E = encoding; M = Maintenance.

Mapping Of Impaired Network Connectivity In Network 1

As we found decreased connectivity in Network 1 of AD group during retrieval, we further explored node-wise functional connectivity comparison between AD and controls during encoding, maintenance and retrieval respectively. During retrieval, 29 in 56 nodes were found having significantly reduced links (32 edges), and they located in the medial prefrontal cortex, posterior cingulate cortex, middle temporal and inferior parietal cortex of left hemisphere, as well as inferior temporal and medial prefrontal cortex of right hemisphere. The majority of nodes with reduced connectivity were assigned to DMN (yellow balls in Fig. 5), followed by the limbic network and FPN (blue and green balls in Fig. 5). In the maintenance, only 16 in 56 nodes were found with reduced links (21 edges) in AD. The reduced connectivity had a similar pattern as that in the retrieval phase, predominantly in the DMN of the left hemisphere. During encoding, we observed only 10 nodes with 9 reduced links in AD (Fig. 5).

Each row represents reduced Network 1-Network 1 connectivity in AD compared to controls in each phase. Significant effects are visualized as a set of binary links. The nodes with significant connectivity changes are colored by its *priori* network assignments in the Schaefer atlas. Larger sized nodes indicate significant decreased functional entropy in the AD, overlapping with decreased functional connectivity

here. DMN = default mode network; FPN = frontoparietal network; DAN = dorsal attention network; VAN = ventral attention network.

To elucidate the nature of the reduced connectivity in AD, we investigated entropy as a measure of BOLD time series predictability (24). To that end, we computed the entropy-based measure (SampEn) in AD and controls. For completeness, we extract time series in all nodes (encoding, maintenance and retrieval phases respectively) and conducted node-wise comparisons between two groups. The p values were corrected by Benjamini/Hochberg false discovery rate at the level of 0.05 in each phase. The AD showed reduced entropy in 5 nodes (temporal pole, olfactory cortex, medial prefrontal cortex and inferior prefrontal cortex in the left and cingulate cortex in the right hemisphere), which were all in the Network 1 during retrieval phase. Except left temporal pole, four nodes among them had reduced functional connectivity in AD (showed as larger nodes in Fig. 5). The results indicated that decreased functional connectivity appears to be partially characterized by more regular and predictable BOLD time series in AD during information retrieval.

Relationship Between Cortical Aβ And Functional Connectivity

There was a positive relationship between global cortical Aβ and Network 1 connectivity (R = -0.247 [-0.453, -0.016], df = 70, p = 0.032) during retrieval, which remained significant after 10,000 permutations. This relationship was not present for Network 1 connectivity during encoding or maintenance (R = -0.113 [-0.336, 0.122], df = 70, p = 0.336; R = -0.142 [-0.362, 0.009], df = 70, p = 0.228). To investigated the spatial specificity, we also evaluated the correlations between Network 1 connectivity in the retrieval phase and averaged cortical Aβ in the Network 1–3 nodes. Only the global cortical amyloid had a robust adverse impact on Network 1 connectivity. There was no relationship between global cortical amyloid and connectivity in Network 2, Network 3, Network 1–2 and Network 2–3 in any memory phases (Fig. 6).

The cortical Aβ deposition were associated with Network 1-Network 1 functional connectivity in the retrieval phase. No other associations were observed. R and P_{corr} represented correlation coefficient and significance across two groups. P_{corr} in the correlation analysis was corrected by 10,000 permutations. The grey zone around blue lines represents the 95% confidence interval for predictions from the linear model. surfsuvr = surface standardized uptake value ratios; N1_1 = Network 1-Network 1; N2_2 = Network 2-Network 2; N3_3 = Network 3-Network 3; N1_3 = Network 1-Network 3; N2_3 = Network 2-Network 3. R = Retrieval; E = encoding; M = Maintenance.

Relationship Between Cortical Aβ And Memory

After adjusted for age, sex and education by linear regression (variables were transformed into z scores here), there was a negative relationship between cortical Aβ and ACER memory performance (β = -0.44, SE = 0.107, *p* = 0.001). This relationship was kind of less significant and strong for MoCA (β = -0.34, SE =

0.112, $p = 0.003$) and ACER (β = -0.30, SE = 0.114, $p = 0.011$). Mediation analysis indicated that the effect of Aβ on memory performance is mediated through the direct effect of Aβ on Network 1 connectivity during retrieval: average causal mediation effect (ACME) = -0.05 [-0.13, -0.01], $p = 0.035$ (Fig. 7). The mediation effect remains significant at $p = 0.032$ for ACER. As expected, there was no significant mediation effect when the mediator variable was connectivity within the Network 2, Network 3 or between Network 1–3.

Greater cortical Aβ deposition has a significant but indirect association with worse memory performance, mediated via connectivity during retrieval within the Network1. Mediation effects were computed by 10,000 bootstrapped samples and the 95% confidence intervalw were reported. N1_1 = Network 1-Network 1; R = Retrieval.

Relationship Between Cortical Aβ And Task-related Activation

Our results support the conclusion that global cortical amyloid is related to functional connectivity reduction in Network 1 for AD during memory retrieval, as well as memory performance. For completeness, we conducted an additional analysis to test relationship between Aβ and inter-individual differences in accuracy-related BOLD activation during retrieval derived from standard fMRI GLM analysis. We found strong evidence for BOLD modulation by global cortical amyloid deposition as negative linear relationship (mean amyloid and BOLD activation: R = -0.365 [-0.550, -0.147], $p = 0.001$), while not specific to local cortical amyloid in the activation region (local amyloid and BOLD activation: R = -0.267 [-0.470, -0.038], $p = 0.023$).

Discussion

We found that AD participants were mainly characterized by decreased functional connectivity in the Network 1 community (dominantly composed of DMN, limbic network and FPN) during the maintenance and retrieval phase in the memory task. Within Network 1, AD had more nodes with reduced connectivity during the retrieval phase than other phases, and the nodes located in the medial prefrontal cortex, posterior cingulate cortex, middle temporal and inferior parietal cortex of left hemisphere, as well as inferior temporal and medial prefrontal cortex of right hemisphere. The novel contribution of the study is the demonstration that global cortical Aβ was associated with reduction in Network 1 connectivity only during retrieval. The mediation analysis indicated that cortical Aβ might affect memory performance by modulating retrieval relevant functional connectivity within the Network 1.

Network 1 Connectivity Is Predominantly Impaired In Ad

As memory maintenance is believed to require the coordination of more neocortex regions (27–29), we clustered regions with assignments to *priori* networks based on functional connectivity during the

maintenance phase. Although Network 1 was composed of four *priori* networks, and its regions were spatially well-organized in the bilateral temporal cortex, medial prefrontal cortex, posterior cingulate cortex and occipitotemporal regions (Fig. 2). The pattern of Network 1 is like the joint of the anterior-temporal and posterior-medial system (30), which work interactively for encoding and retrieval memory (31, 32). The reduced functional connectivity within Network 1 is consistent with evidence found in resting-state fMRI, both in AD and cognitively unimpaired amyloid-β + individuals (22, 33). Importantly, we found the reduction specifically in the maintenance and retrieval phase of memory. As in our previous work, retrieval deficiencies could be the cause of poor performance (5). An intervention study provided additional evidence for the importance of the retrieval phase in recognition (34). Taken together, these suggested that Network 1 successfully clustered regions that were working together for memory maintenance and retrieval, and it was impaired in AD.

Functional connectivity within empirical networks is related to memory performance

We report significant positive correlations between the Network 1 connectivity and ACER memory performance in encoding, maintenance and retrieval phases. Compared to similar positive relationships between memory and the Network 2 and Network 3 in some phases, Network 1 connectivity correlated with memory more steadily and strongly during all phases. As the dominant role of DMN in Network 1, these results are consistent with studies that highlight the importance of DMN activation (35) and cortical network reorganization for better cognitive performance (36, 37), especially when large shifts of attention are required during cognitive operations.

Note that the task accuracy-related activation during retrieval was located in the left superior frontal cortex, within VAN/Network 2. In the working memory model, retrieval requires phonological loop and central executive, which is generally defined as attention allocation efficiency (38, 39). In our study, the task accuracy also correlated with memory performance, suggesting the failure to recruit the VAN may also hamper the cognitively demanding selection.

Impaired Node-wise Connectivity During Memory Phases

As we found the hallmark of the AD group had decreased connectivity in Network 1 during retrieval, we further explored node-wise functional connectivity comparison. As expected from the above results, more nodes had different connectivity during the retrieval phase than other phases. Some nodes were clustered in the left posterior cingulate cortex, originally assigned to left DMN. During a memory process, the functional connectivity between DMN sub-networks increases in the retrieval of episodic memories (40). In AD, reduced resting-state functional connectivity was observed in posterior DMN nodes as precuneus/posterior cingulate cortex (41). Besides, we observed another hub in the DMN, medial prefrontal cortex, with reduced connectivity. Similarly, previous research on the schema memories showed

the activation of the mPFC associated with successful memory for schema items (42). Importantly, our results appeared to be strongly left-lateralized in the retrieval phase. This fits with earlier studies showing similar left-lateralized effects in early Alzheimer's disease using resting-state fMRI (22), volumetric grey matter measurements (43), FDG-PET (44) or amyloid PET (45).

To elucidate the nature of decreased functional connectivity in AD, we calculated node-wise entropy in Network 1. Nodes with reduced entropy (i.e. reduced BOLD signal predictability) showed clear spatial correspondence with nodes of reduced connectivity relative to CN, only during the retrieval phase. This indicates that some regions in Network 1 with decreased functional connectivity are more predictable and less random with reduced complexity. The results revealed retrieval related connectivity-entropy coupling and showed difference in AD from normal aging (24).

The Relationship Between β-amyloid, Memory And Cortical Activity

We find a negative correlation between cortical amyloid and ACER memory performance. Our findings were consistent with previous amyloid studies, which found that higher amyloid deposition correlated with lower immediate memory and delayed recall scores in MCI participants and amyloid-positive healthy controls (46, 47).

It was once argued that amyloid pathology and neurodegeneration have adverse, in part synergistic, effects on prospective cognition (48). In addition to the linear relationship found between Aβ and cognition (49), Aβ load was revealed for its nonlinear role in moderating the BOLD activation effect on behavioral task performance (50, 51). Taken together, these findings suggested the involvement but lack of direct and consistent effect of Aβ on the cognitive deficiency. Several of our results are in accordance with this hypothesis. First, the correlation between cortical amyloid and memory performance/task activation was not regionally specific. Second, the negative correlation between cortical Aβ and Network 1 connectivity was significant only in the retrieval phase. Third, the mediation analyses indicated a significant effect of Aβ on memory performance, mediated through a direct effect on Network 1 connectivity during the retrieval phase. Furthermore, we report no significant relationships between Aβ and Network 2 or 3 connectivity change, or Network 1 during other phases.

These results also suggested that global cortical amyloid might exert an influence on memory performance through an effect on functional connectivity during memory retrieval within the Network 1, which mainly included DMN, limbic network and FPN. Participants with higher cortical amyloid deposition exhibited the pronounced Network 1 connectivity decrease, which predicted worse memory performance.

Limitations

Our study has some strengths that extend the current literature, including measurement of cortical amyloid, connectivity, entropy in the same participants, and examination of memory phase-locked functional connectivity. One key limitation is that it is not possible to make strong inferences regarding the direction of causality from purely observational studies. Related to this, there may be (unmeasured) biomarkers (e.g tau) and neuronal variables, which exert a more direct causal influence on memory performance. These concerns can only be addressed in fully randomized interventional experimental designs. Second, as we did not find regionally specific effects from amyloid, our findings are the result of the global effects of Alzheimer's disease pathology in the cortex. We cannot be sure which regions are more vulnerable to local pathological change.

Conclusion

We employ a multimodal neuroimaging approach to test the relationship between cortical amyloid and memory performance in AD and controls. Taken together, our results suggest that mean cortical Aβ deposition is directly related to Network 1 functional connectivity decrease during memory retrieval, and that greater reductions are associated with worse memory performance. In a mediation analysis, we show that cortical Aβ may impair memory performance through its relationship with Network 1 connectivity during memory retrieval. These findings help mapping impaired functional connectivity during memory phases and explain memory deficiency due to cortical Aβ in AD patients.

List Of Abbreviations

AD, Alzheimer's disease; PET, positron emission tomography; MRI, magnetic resonance imaging; β-amyloid (Aβ); MMSE, Mini-Mental State Examination; CDR, global clinical dementia rating; MoCA, Montreal Cognitive Assessment; ACER, Addenbrooke's Cognitive Examination-Revised; FWHM, full-width half-maximum; GLM, general linear model; BOLD, Blood oxygen level-dependent; DAN, dorsal attention network; VAN, ventral attention network; FPN, frontoparietal network; DMN, default mode network; SUVR, standardized uptake value ratios.

Declarations

Ethics approval and consent to participate

The collection and analysis was approved by the Ethics Committee, Shanghai Jiao Tong University affiliated Ruijin Hospital, China.

Consent for publication

Not applicable

Availability of data and materials

Anonymized data will be shared by request from a qualified academic investigator for the sole purpose of replicating procedures and results presented in the article.

Competing interests

The authors declare that they have no competing interests

Funding

This study was supported by National Key Research and Development Program (2016YFC1306505); the National Natural Science Foundation of China (81873778); the Science and Technology Commission of Shanghai Municipality (18JC1420303); the Three-year planning of Shanghai Shen-Kang Promoting Hospital's Clinical Skills and Innovative Ability Project (16CR3110B); Shanghai Municipal Key Clinical Specialty (shslczdzk03403). The authors declare that they have no conflict of interest relevant to this article.

Author's contributions

ByL analyzed and interpreted all imaging data and drafted the manuscript. MZ performed PET-MR and was the equal contributor in writing the manuscript. Xz L, Hp M and Xy H performed PET-MR scanning. Wx H synthesized AV45 tracer. Gy Y, LcZ and Gy H helped clinical data collection. Sd C supervised the research. BL and JL supervised, reviewed and modified the manuscript. All authors read and approved the final manuscript.

Acknowledgements

We would like to thank our anonymous reviewers for thoughtful comments on the manuscript. We are also grateful to all research participants. We thank Pro. Hank Kung and Lin Zhu for their kindly gifting of Florbetapir precursor and suggestions to improve this manuscript. We are also grateful to all of the study participants for their patience and cooperation.

Declaration of Competing Interests

None

References

1. Pasquier F, Grymonprez L, Lebert F, Van der Linden M. Memory impairment differs in frontotemporal dementia and Alzheimer's disease. Neurocase. 2001;7(2):161–71. PubMed PMID: 11320163.
2. Weintraub S, Wicklund AH, Salmon DP. The neuropsychological profile of Alzheimer disease. Cold Spring Harbor perspectives in medicine. 2012 Apr;2(4):a006171. PubMed PMID: 22474609. Pubmed Central PMCID: 3312395.

3. Grober E, Kawas C. Learning and retention in preclinical and early Alzheimer's disease. Psychology aging. 1997 Mar;12(1):183–8. PubMed PMID: 9100279.
4. Albert MS, Moss MB, Tanzi R, Jones K. Preclinical prediction of AD using neuropsychological tests. Journal of the International Neuropsychological Society: JINS. 2001 Jul;7(5):631–9. PubMed PMID: 11459114.
5. Li BY, Tang HD, Chen SD. Retrieval Deficiency in Brain Activity of Working Memory in Amnesic Mild Cognitive Impairment Patients: A Brain Event-Related Potentials Study. Front Aging Neurosci. 2016;8:54. PubMed PMID: 27047371. Pubmed Central PMCID: 4803731.
6. Roy DS, Arons A, Mitchell TI, Pignatelli M, Ryan TJ, Tonegawa S. Memory retrieval by activating engram cells in mouse models of early Alzheimer's disease. Nature. 2016 Mar 24;531(7595):508–12. PubMed PMID: 26982728. Pubmed Central PMCID: 4847731.
7. Mormino EC, Brandel MG, Madison CM, Marks S, Baker SL, Jagust WJ. Aβ Deposition in aging is associated with increases in brain activation during successful memory encoding. Cerebral cortex (New York, NY: 1991). 2012;22(8):1813-23. PubMed PMID: 21945849. Epub 09/23. eng.
8. Vannini P, Hedden T, Becker JA, Sullivan C, Putcha D, Rentz D, et al. Age and amyloid-related alterations in default network habituation to stimulus repetition. Neurobiol Aging. 2012;33(7):1237–52. PubMed PMID: 21334099. Epub 02/18. eng.
9. Aggarwal NT, Wilson RS, Beck TL, Bienias JL, Bennett DA. Mild cognitive impairment in different functional domains and incident Alzheimer's disease. Journal of neurology, neurosurgery, and psychiatry. 2005 Nov;76(11):1479–84. PubMed PMID: 16227534. Pubmed Central PMCID: 1739422.
10. Bostancikliogl M. An update on memory formation and retrieval: An engram-centric approach. Alzheimer's & dementia: the journal of the Alzheimer's Association. 2020 Apr 25. PubMed PMID: 32333509.
11. Tonegawa S, Morrissey MD, Kitamura T. The role of engram cells in the systems consolidation of memory. Nature reviews Neuroscience. 2018 Aug;19(8):485–98. PubMed PMID: 29970909.
12. Jack CR Jr, Bennett DA, Blennow K, Carrillo MC, Dunn B, Haeberlein SB, et al. NIA-AA Research Framework: Toward a biological definition of Alzheimer's disease. Alzheimer's dementia: the journal of the Alzheimer's Association. 2018;14(4):535–62. PubMed PMID: 29653606. eng.
13. Katzman R, Zhang MY, Ouang Ya Q, Wang ZY, Liu WT, Yu E, et al. A Chinese version of the Mini-Mental State Examination; impact of illiteracy in a Shanghai dementia survey. J Clin Epidemiol. 1988;41(10):971–8. PubMed PMID: 3193141.
14. Fang R, Wang G, Huang Y, Zhuang JP, Tang HD, Wang Y, et al. Validation of the Chinese version of Addenbrooke's cognitive examination-revised for screening mild Alzheimer's disease and mild cognitive impairment. Dementia and geriatric cognitive disorders. 2014;37(3–4):223 – 31. PubMed PMID: 24193223..
15. Greve DN, Fischl B. False positive rates in surface-based anatomical analysis. NeuroImage. 2018 May 1;171:6–14. PubMed PMID: 29288131. Pubmed Central PMCID: 5857431.

16. Nour MM, Dahoun T, McCutcheon RA, Adams RA, Wall MB, Howes OD. Task-induced functional brain connectivity mediates the relationship between striatal D2/3 receptors and working memory. eLife. 2019;8.
17. Schaefer A, Kong R, Gordon EM, Laumann TO, Zuo XN, Holmes AJ, et al. Local-Global Parcellation of the Human Cerebral Cortex from Intrinsic Functional Connectivity MRI. Cerebral cortex. 2018 Sep 1;28(9):3095 – 114. PubMed PMID: 28981612. Pubmed Central PMCID: 6095216.
18. Blondel VD, Guillaume J-L, Lambiotte R, Lefebvre E. Fast unfolding of communities in large networks. Journal of statistical mechanics: theory experiment. 2008;2008(10):P10008.
19. Hearne LJ, Cocchi L, Zalesky A, Mattingley JB. Reconfiguration of brain network architectures between resting-state and complexity-dependent cognitive reasoning. J Neurosci. 2017;37(35):8399–411.
20. Cohen JR, D'Esposito M. The segregation and integration of distinct brain networks and their relationship to cognition. J Neurosci. 2016;36(48):12083–94.
21. Zalesky A, Fornito A, Bullmore ET. Network-based statistic: identifying differences in brain networks. NeuroImage. 2010 Dec;53(4):1197–207. PubMed PMID: 20600983.
22. Berron D, van Westen D, Ossenkoppele R, Strandberg O, Hansson O. Medial temporal lobe connectivity and its associations with cognition in early Alzheimer's disease. Brain. 2020 Apr 1;143(4):1233-48. PubMed PMID: 32252068. Pubmed Central PMCID: 7174043.
23. Richman JS, Moorman JR. Physiological time-series analysis using approximate entropy and sample entropy. Am J Physiol Heart Circ Physiol. 2000;278(6):H2039-H49.
24. Yao Y, Lu WL, Xu B, Li CB, Lin CP, Waxman D, et al. The increase of the functional entropy of the human brain with age. Scientific reports. 2013 Oct 9;3:2853. PubMed PMID: 24103922. Pubmed Central PMCID: 3793229.
25. Greve DN, Salat DH, Bowen SL, Izquierdo-Garcia D, Schultz AP, Catana C, et al. Different partial volume correction methods lead to different conclusions: An (18)F-FDG-PET study of aging. NeuroImage. 2016 May 15;132:334 – 43. PubMed PMID: 26915497. Pubmed Central PMCID: 4851886.
26. Lancichinetti A, Fortunato S. Consensus clustering in complex networks. Scientific reports. 2012;2:336. PubMed PMID: 22468223. Pubmed Central PMCID: 3313482.
27. Takahama S, Saiki J. Functional connectivity supporting the selective maintenance of feature-location binding in visual working memory. Frontiers in psychology. 2014;5:507. PubMed PMID: 24917833. Pubmed Central PMCID: 4040507.
28. Woodward TS, Cairo TA, Ruff CC, Takane Y, Hunter MA, Ngan ET. Functional connectivity reveals load dependent neural systems underlying encoding and maintenance in verbal working memory. Neuroscience. 2006 Apr 28;139(1):317–25. PubMed PMID: 16324799.
29. Gazzaley A, Rissman J, D'Esposito M. Functional connectivity during working memory maintenance. Cognitive, affective & behavioral neuroscience. 2004 Dec;4(4):580–99. PubMed PMID: 15849899.

30. Libby LA, Ekstrom AD, Ragland JD, Ranganath C. Differential connectivity of perirhinal and parahippocampal cortices within human hippocampal subregions revealed by high-resolution functional imaging. J Neurosci. 2012;32(19):6550–60.
31. Cooper RA, Ritchey M. Cortico-hippocampal network connections support the multidimensional quality of episodic memory. Elife. 2019;8:e45591.
32. Collins JA, Dickerson BC. Functional connectivity in category-selective brain networks after encoding predicts subsequent memory. Hippocampus. 2019;29(5):440–50.
33. Harrison TM, Maass A, Adams JN, Du R, Baker SL, Jagust WJ. Tau deposition is associated with functional isolation of the hippocampus in aging. Nature communications. 2019;10(1):1–12.
34. Smith JC, Nielson KA, Antuono P, Lyons JA, Hanson RJ, Butts AM, et al. Semantic memory functional MRI and cognitive function after exercise intervention in mild cognitive impairment. Journal of Alzheimer's disease: JAD. 2013;37(1):197–215. PubMed PMID: 23803298. Pubmed Central PMCID: 4643948.
35. Smith V, Mitchell DJ, Duncan J. Role of the Default Mode Network in Cognitive Transitions. Cerebral cortex. 2018 Oct 1;28(10):3685-96. PubMed PMID: 30060098. Pubmed Central PMCID: 6132281.
36. Shine JM, Poldrack RA. Principles of dynamic network reconfiguration across diverse brain states. NeuroImage. 2018 Oct 15;180(Pt B):396–405. PubMed PMID: 28782684.
37. Shine JM, Bissett PG, Bell PT, Koyejo O, Balsters JH, Gorgolewski KJ, et al. The Dynamics of Functional Brain Networks: Integrated Network States during Cognitive Task Performance. Neuron. 2016 Oct 19;92(2):544–54. PubMed PMID: 27693256. Pubmed Central PMCID: 5073034.
38. Germano C, Kinsella GJ. Working memory and learning in early Alzheimer's disease. Neuropsychology review. 2005 Mar;15(1):1–10. PubMed PMID: 15929495.
39. Wang Y, Song Y, Qu Z, Ding Y. Task difficulty modulates electrophysiological correlates of perceptual learning. International journal of psychophysiology: official journal of the International Organization of Psychophysiology. 2010 Mar;75(3):234–40. PubMed PMID: 19969030.
40. Sestieri C, Corbetta M, Romani GL, Shulman GL. Episodic memory retrieval, parietal cortex, and the default mode network: functional and topographic analyses. J Neurosci. 2011 Mar 23;31(12):4407-20. PubMed PMID: 21430142. Pubmed Central PMCID: 3098040.
41. Badhwar A, Tam A, Dansereau C, Orban P, Hoffstaedter F, Bellec P. Resting-state network dysfunction in Alzheimer's disease: a systematic review and meta-analysis. Alzheimer's & Dementia: Diagnosis, Assessment & Disease Monitoring. 2017;8:73–85.
42. Liu ZX, Grady C, Moscovitch M. Effects of Prior-Knowledge on Brain Activation and Connectivity During Associative Memory Encoding. Cerebral cortex. 2017 Mar 1;27(3):1991–2009. PubMed PMID: 26941384.
43. Shi F, Liu B, Zhou Y, Yu C, Jiang T. Hippocampal volume and asymmetry in mild cognitive impairment and Alzheimer's disease: Meta-analyses of MRI studies. Hippocampus. 2009 Nov;19(11):1055–64. PubMed PMID: 19309039.

44. Weise CM, Chen K, Chen Y, Kuang X, Savage CR, Reiman EM, et al. Left lateralized cerebral glucose metabolism declines in amyloid-beta positive persons with mild cognitive impairment. NeuroImage Clinical. 2018;20:286 – 96. PubMed PMID: 30101060. Pubmed Central PMCID: 6084012..
45. Raji CA, Becker JT, Tsopelas ND, Price JC, Mathis CA, Saxton JA, et al. Characterizing regional correlation, laterality and symmetry of amyloid deposition in mild cognitive impairment and Alzheimer's disease with Pittsburgh Compound B. Journal of neuroscience methods. 2008 Jul 30;172(2):277 – 82. PubMed PMID: 18582948. Pubmed Central PMCID: 2501111.
46. Doraiswamy PM, Sperling RA, Coleman RE, Johnson KA, Reiman EM, Davis MD, et al. Amyloid-beta assessed by florbetapir F 18 PET and 18-month cognitive decline: a multicenter study. Neurology. 2012 Oct 16;79(16):1636-44. PubMed PMID: 22786606. Pubmed Central PMCID: 3468774.
47. Sperling RA, Johnson KA, Doraiswamy PM, Reiman EM, Fleisher AS, Sabbagh MN, et al. Amyloid deposition detected with florbetapir F 18 ((18)F-AV-45) is related to lower episodic memory performance in clinically normal older individuals. Neurobiol Aging. 2013;34(3):822–31. PubMed PMID: 22878163. Epub 08/09. eng.
48. Bilgel M, An Y, Helphrey J, Elkins W, Gomez G, Wong DF, et al. Effects of amyloid pathology and neurodegeneration on cognitive change in cognitively normal adults. Brain. 2018 Aug 1;141(8):2475-85. PubMed PMID: 29901697. Pubmed Central PMCID: 6061788.
49. Knopman DS, Lundt ES, Therneau TM, Vemuri P, Lowe VJ, Kantarci K, et al. Joint associations of beta-amyloidosis and cortical thickness with cognition. Neurobiology of aging. 2018 May;65:121–31. PubMed PMID: 29471214. Pubmed Central PMCID: 5871603.
50. Foster CM, Kennedy KM, Horn MM, Hoagey DA, Rodrigue KM. Both hyper- and hypo-activation to cognitive challenge are associated with increased beta-amyloid deposition in healthy aging: A nonlinear effect. NeuroImage. 2018 Feb 1;166:285 – 92. PubMed PMID: 29108941. Pubmed Central PMCID: 5747976.
51. Kennedy KM, Foster CM, Rodrigue KM. Increasing beta-amyloid deposition in cognitively healthy aging predicts nonlinear change in BOLD modulation to difficulty. NeuroImage. 2018 Dec;183:142–9. PubMed PMID: 30102997. Pubmed Central PMCID: 6197922.

Additional File Legend

File name: Additional file 1

File format: .docx

Title of data: Supplementary methods

Description of data: Detailed information of the methods

Figures

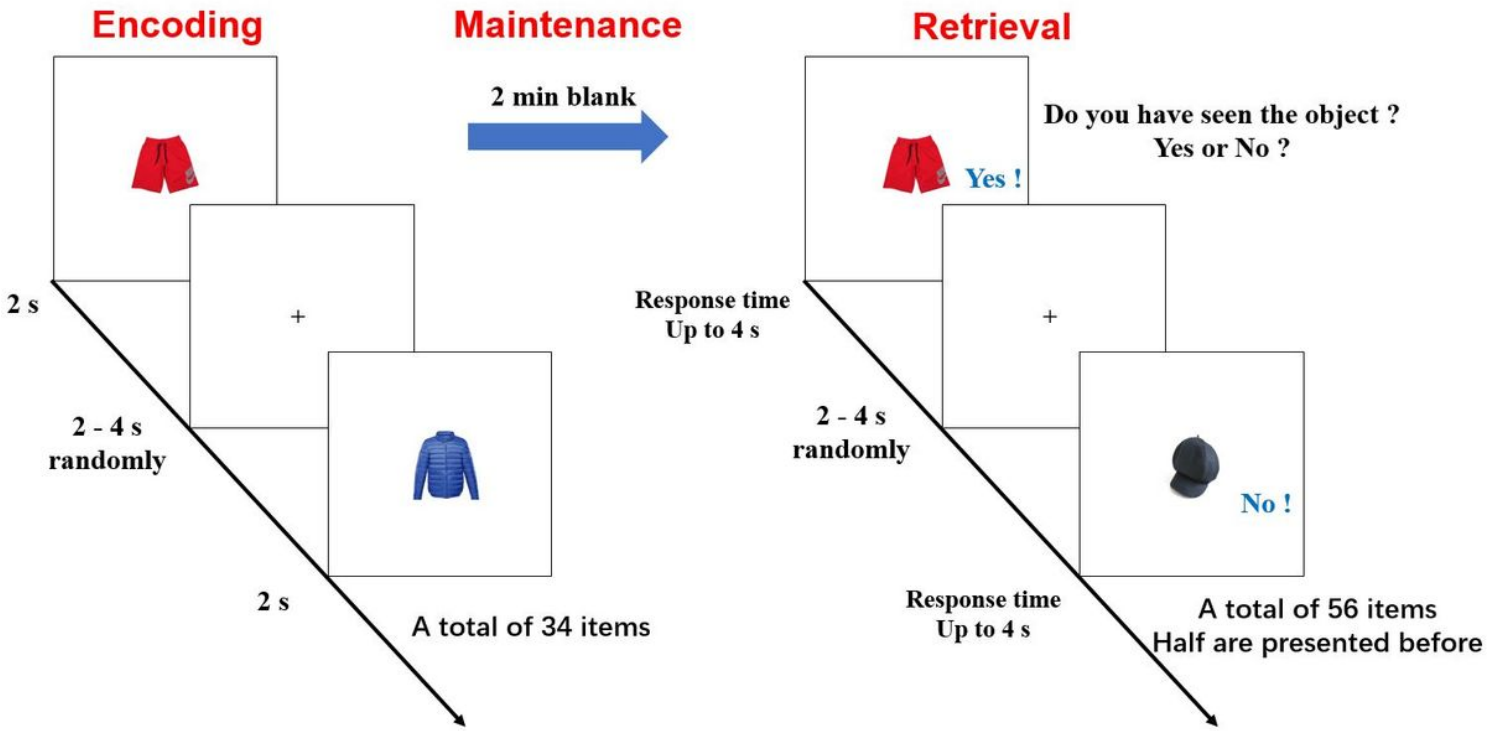

Figure 1

Task design in fMRI. The memory task in the fMRI study, including encoding, blank (memory maintenance), and retrieval phases. In the encoding phase, 34 objects were sequentially presented for 2 seconds respectively. After 2-min blank, the participants indicated, as quickly as possible, whether the object was present or absent in the encoding phase, using two buttons of an MR-compatible button box. During retrieval, each object appeared on the screen until the response or up to 4 s before the next letter was shown. The inter-object interval was randomly set between 2 to 4 s.

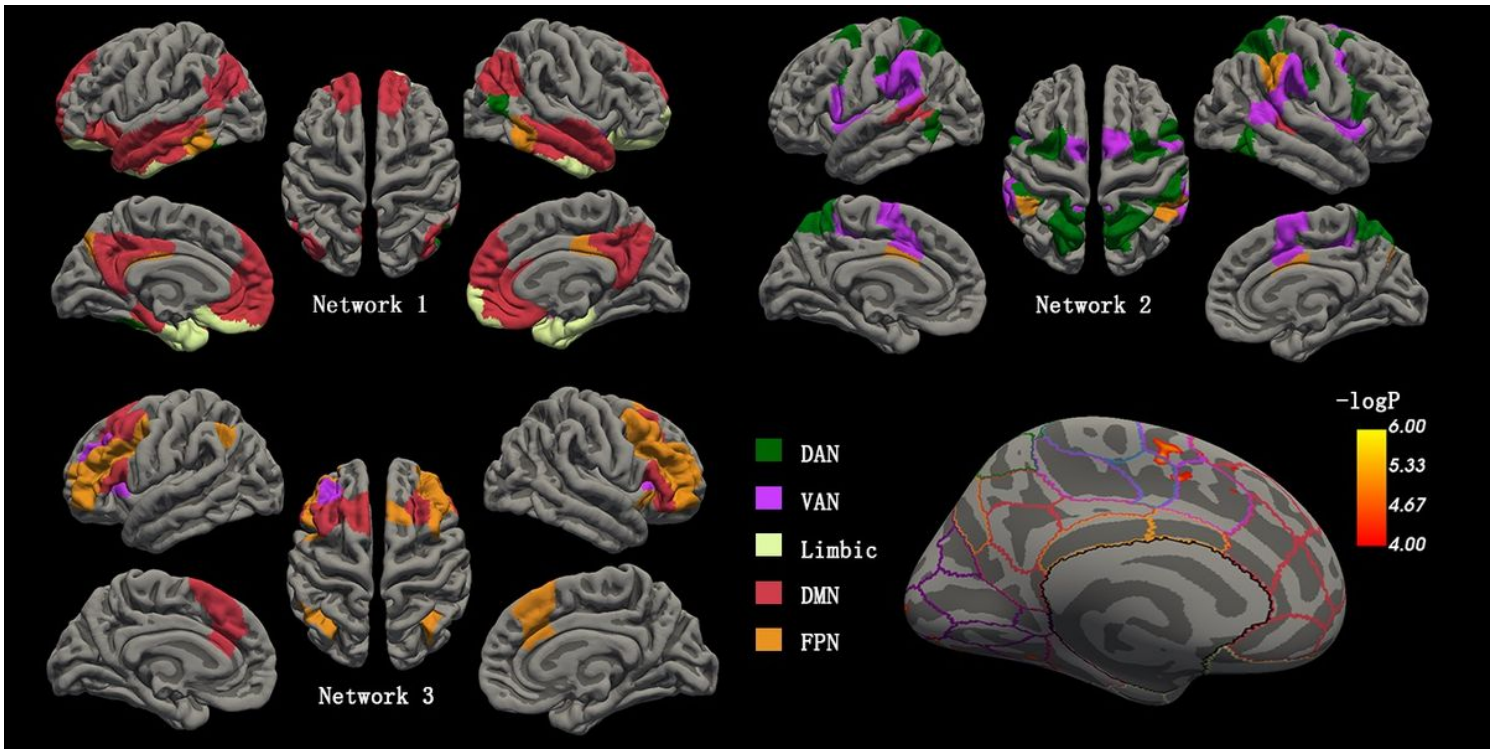

Figure 2

Cortical networks during the maintenance phase and accuracy-related neural activation. Left top, right top and left down cortical mapping illustrated nodes of the three empirical networks identified by the community detection algorithm during the maintenance phase, colored by a priori network assignments from the Schaefer cortical parcellation. Network 1 is mainly composed of DMN and limbic network, and Network 2 consists of DMN and FPN. The Network 3 generally includes DAN and VAN. The right down is the surface maps of the activated cortex in the retrieval phases related to accuracy. The border on the surface indicated the network identical to the above Schaefer cortical parcellation. The activation is observed in the region of VAN. DMN = default mode network; FPN = frontoparietal network; DAN = dorsal attention network; VAN = ventral attention network.

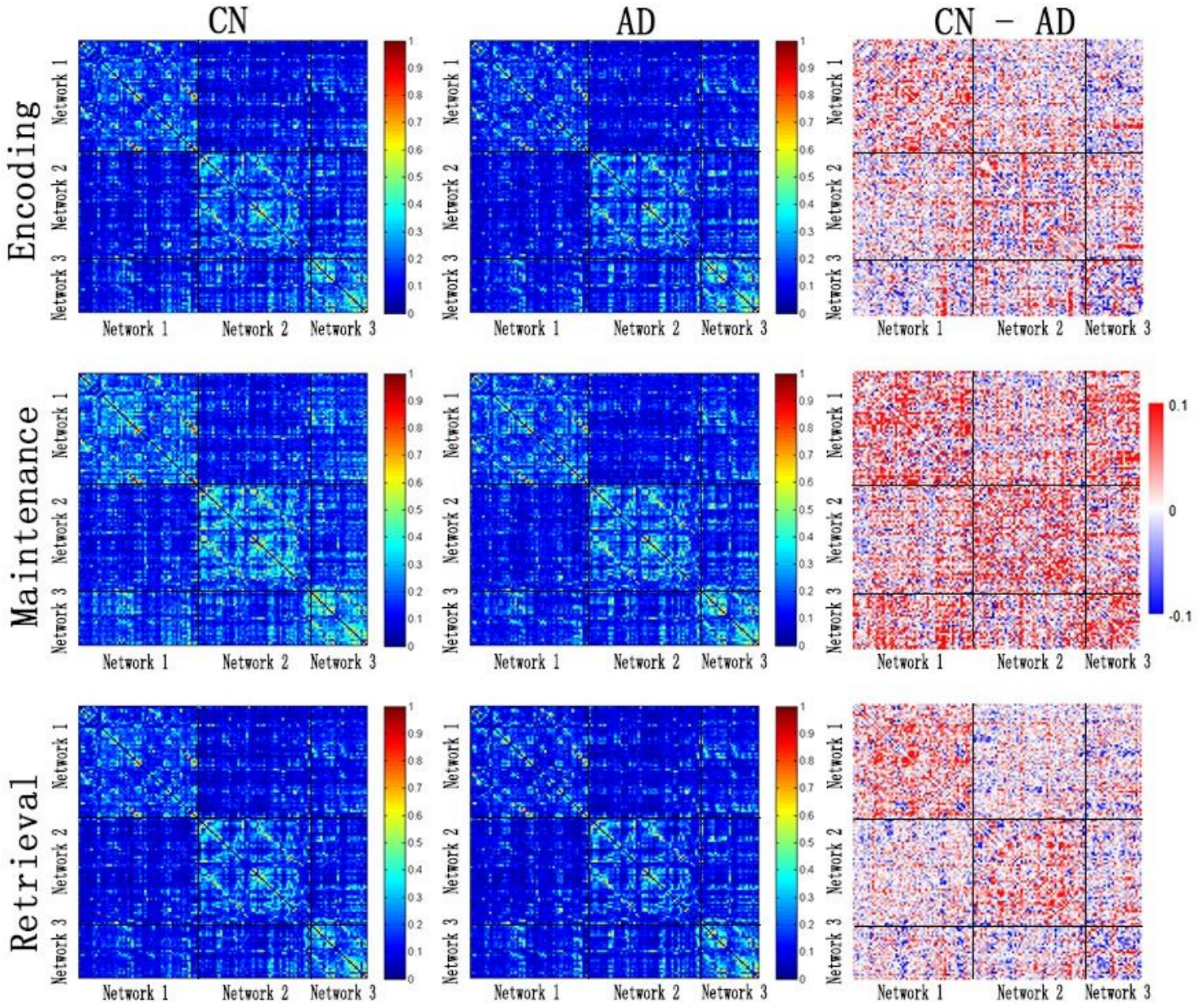

Figure 3

Task phase-locked functional connectivity in AD and controls. Reduced Network 1-Network 1 functional connectivity in AD only during the retrieval phase. The first and second columns: Mean functional connectivity in each task phase of network edge (node-node connection) in the AD and controls. Each edge (cell of the matrix) represents the functional connectivity strength (Fisher z-transformed r-value) within and between the Network 1-3. The third column: The difference of functional connectivity in each task phase of each network edge (node-node connection) between the AD and controls. Black lines indicate the boundary separating nodes allocated to the empirical Network 1-3.

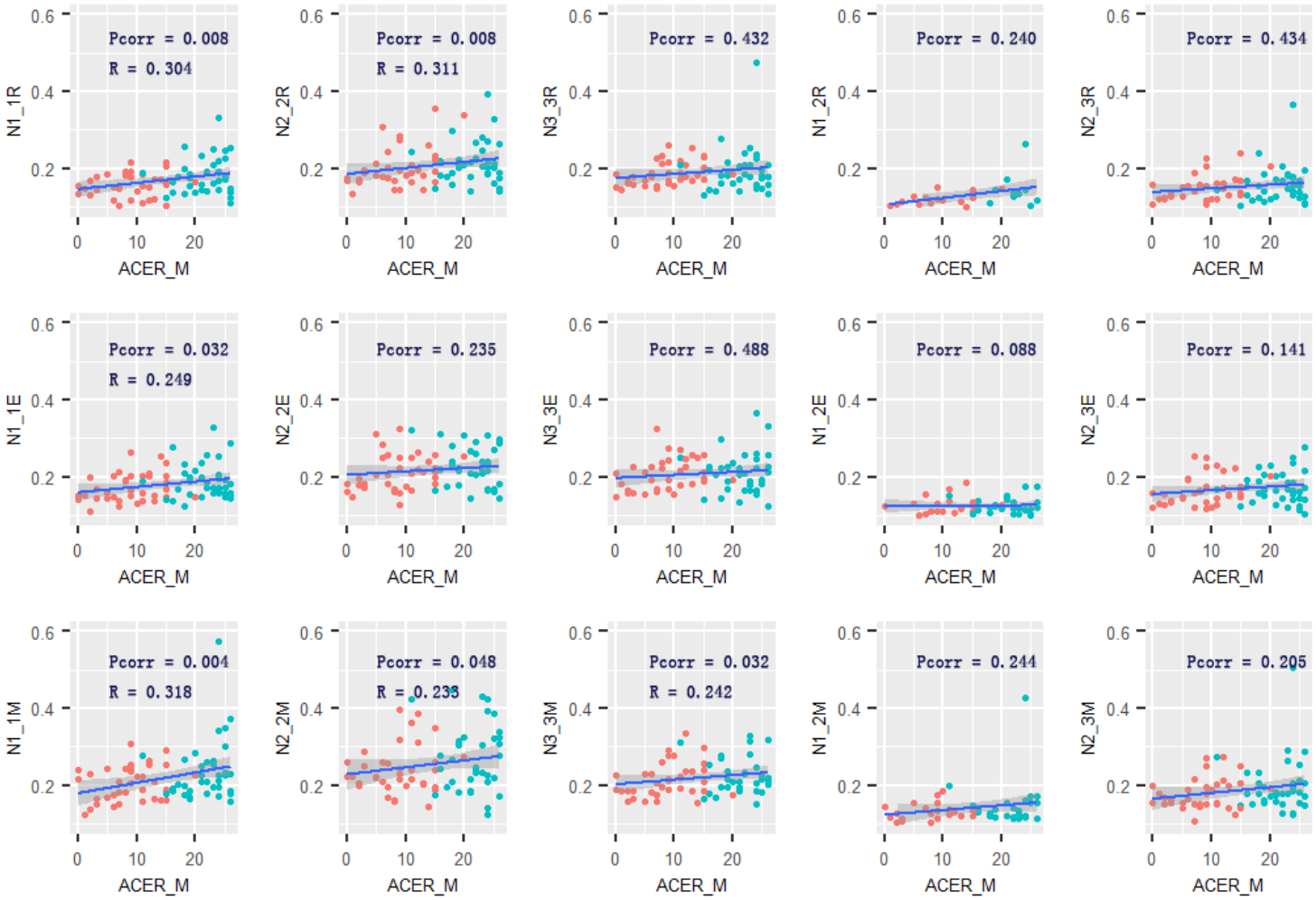

Figure 4

Relationship of memory scores and Network 1-3 connectivity estimates Memory scores in ACER were associated with Network 1-Network 1 functional connectivity in the encoding, maintenance and retrieval phase, while only associated with Network 2-Network 2 functional connectivity in the maintenance and retrieval phase. No other associations were observed. R and Pcorr represented correlation coefficient and significance across two groups. Pcorr in the correlation analysis was corrected by 10,000 permutations. The grey zone around blue lines represents the 95% confidence interval for predictions from the linear model. ACER_M = Addenbrooke's Cognitive Examination-Revised Memory; N1_1 = Network 1-Network 1; N2_2 = Network 2-Network 2; N3_3 = Network 3-Network 3; N1_3 = Network 1-Network 3; N2_3 = Network 2-Network 3. R = Retrieval; E = encoding; M = Maintenance.

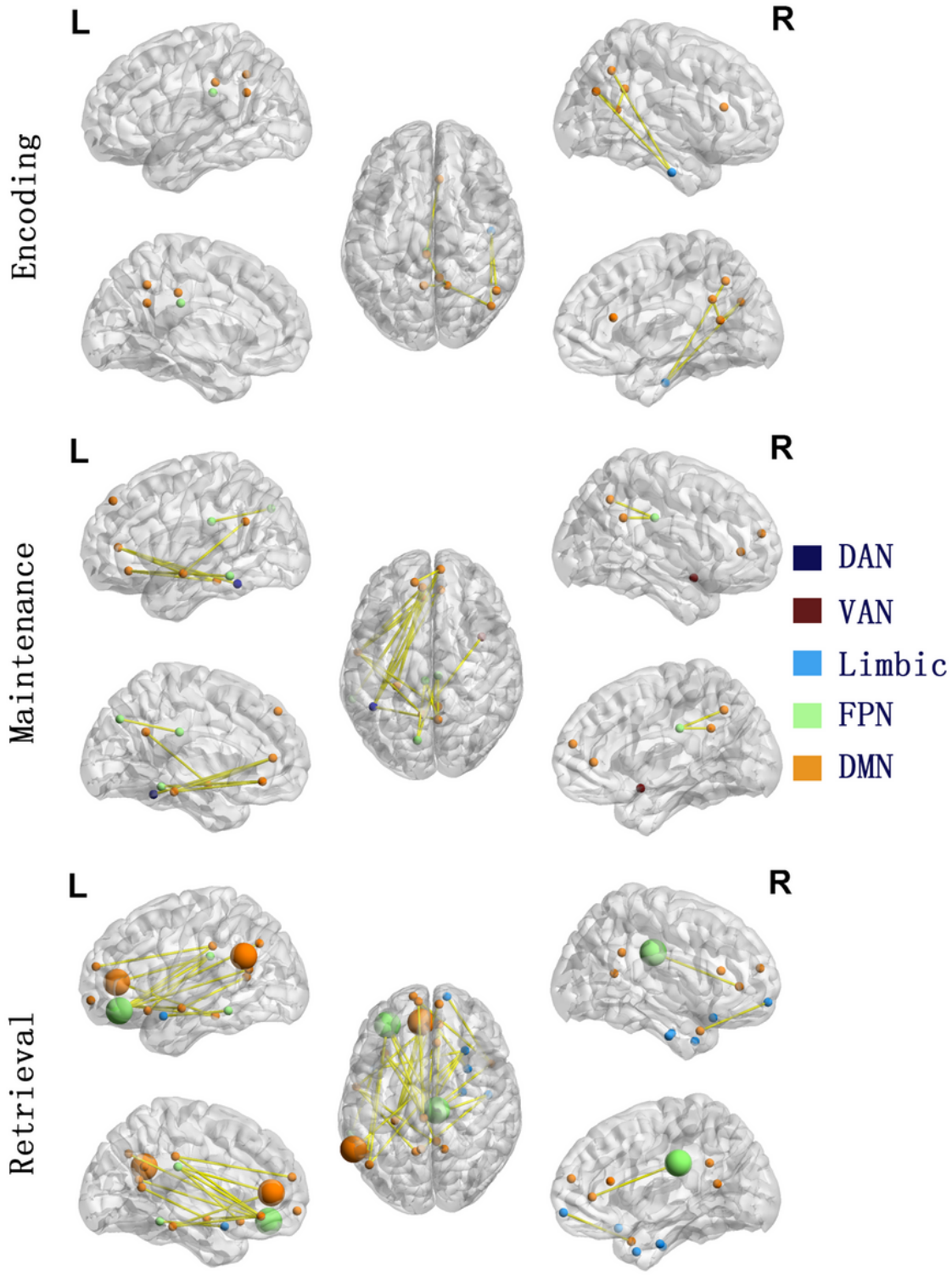

Figure 5

Changes in Network 1-Network 1 functional connectivity. Each row represents reduced Network 1-Network 1 connectivity in AD compared to controls in each phase. Significant effects are visualized as a set of binary links. The nodes with significant connectivity changes are colored by its priori network assignments in the Schaefer atlas. Larger sized nodes indicate significant decreased functional entropy

in the AD, overlapping with decreased functional connectivity here. DMN = default mode network; FPN = frontoparietal network; DAN = dorsal attention network; VAN = ventral attention network.

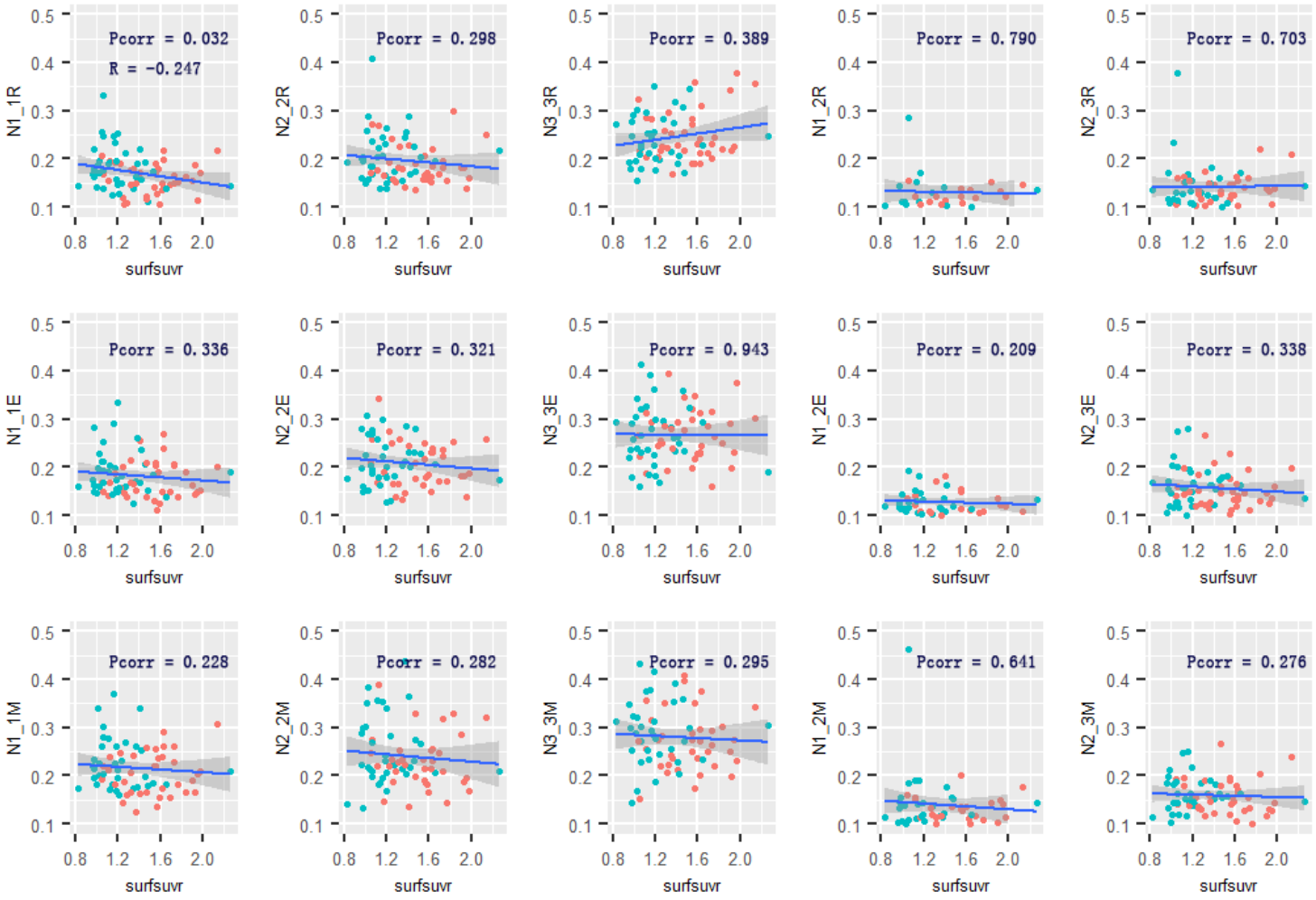

Figure 6

Relationship of cortical amyloid and Network 1-3 connectivity estimates The cortical amyloid deposition were associated with Network 1-Network 1 functional connectivity in the retrieval phase. No other associations were observed. R and Pcorr represented correlation coefficient and significance across two groups. Pcorr in the correlation analysis was corrected by 10,000 permutations. The grey zone around blue lines represents the 95% confidence interval for predictions from the linear model. surfsuvr = surface standardized uptake value ratios; N1_1 = Network 1-Network 1; N2_2 = Network 2-Network 2; N3_3 = Network 3-Network 3; N1_3 = Network 1-Network 3; N2_3 = Network 2-Network 3. R = Retrieval; E = encoding; M = Maintenance.

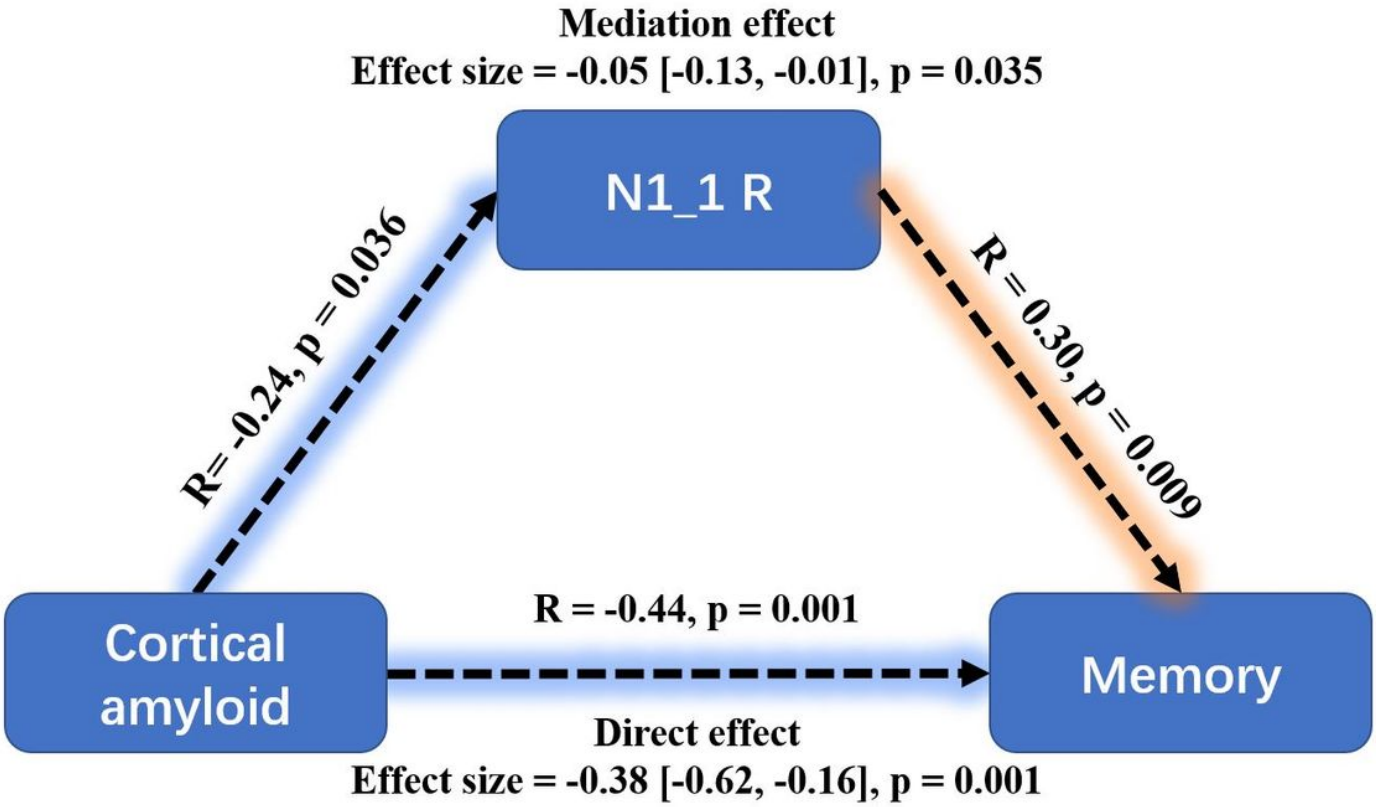

Figure 7

Mediation analysis between cortical amyloid, task related Network1 connectivity, and memory performance Greater cortical amyloid deposition has a significant but indirect association with worse memory performance, mediated via connectivity during retrieval within the Network1. Mediation effects were computed by 10,000 bootstrapped samples and the 95% confidence intervalw were reported. N1_1 = Network 1-Network 1; R = Retrieval.

Supplementary Files

This is a list of supplementary files associated with this preprint. Click to download.

- additionalfile.docx